Received: 31 January 2020 | Revised: 6 April 2020 | Accepted: 26 April 2020

DOI: 10.1002/aoc.5896

FULL PAPER

Applied Organometallic Chemistry WILEY

Ruthenium tetrazene complexes bearing glucose moieties on their periphery: Synthesis, characterization, and *in vitro* cytotoxicity

Vojtěch Hamala[1,2] | Andrea Martišová[3] | Lucie Červenková Šťastná[1] | Jindřich Karban[1] | Andrej Dančo[4] | Adam Šimarek[4] | Martin Lamač[4] | Michal Horáček[4] | Tamara Kolářová[3] | Roman Hrstka[3] | Róbert Gyepes[4,5] | Jiří Pinkas[4]

[1]Academy of Sciences of the Czech Republic, Institute of Chemical Process Fundamentals, v.v.i., Rozvojová 135, Prague 6, 165 02, Czech Republic

[2]Faculty of Chemical Technology, University of Chemistry and Technology Prague, Technická 5, Prague 6, 166 28, Czech Republic

[3]Regional Centre for Applied and Molecular Oncology, Masaryk Memorial Cancer Institute, Žlutý kopec 7, Brno, 65653, Czech Republic

[4]Academy of Sciences of the Czech Republic, J. Heyrovský Institute of Physical Chemistry, v.v.i., Dolejškova 2155/3, Prague 8, 182 23, Czech Republic

[5]Department of Inorganic Chemistry, Charles University, Hlavova 2030, Prague 2, 128 43, Czech Republic

Correspondence
Jiří Pinkas, J. Heyrovský Institute of Physical Chemistry, Academy of Sciences of the Czech Republic, v.v.i., Dolejškova 2155/3, 182 23 Prague 8, Czech Republic.
Email: jiri.pinkas@jh-inst.cas.cz

Funding information
Grantová Agentura České Republiky, Grant/Award Number: 17-05838S; Ministerstvo Zdravotnictví Ceské Republiky, Grant/Award Number: DRO MMCI, 00209805; Ministry of Health of the Czech Republic; the Czech Science Foundation

Ruthenium tetrazene complexes with general formula [Cp*RuCl(1,4-R_2N_4)] (Cp* = η^5-C_5Me_5), where R = benzyl (**1**), 2-fluorobenzyl (**2**), β-D-glucopyranosyl-unprotected (**3a**) and acyl-protected (**3b–d**), 2-acetamido-β-D-glucopyranosyl-unprotected (**4a**) and acyl-protected (**4b–d**), propyl-β-D-glucopyranoside-unprotected (**5a**), and *O*-acetylated (**5b**), were synthesized and characterized using nuclear magnetic resonance and electrospray ionization–mass spectrometry. In addition, the molecular structure of **3b** was determined using X-ray crystallography. The cytotoxicity of complexes against ovarian (A2780, SK-OV-3) and breast (MDA-MB-231) cancer cell lines and non-cancerous cell line HEK-293 was evaluated and compared to cisplatin activity. The carbohydrate-modified complexes bearing acyl-protecting groups exhibited higher efficacy (in low micromolar range) than unprotected ones, where the most active **4d** was superior to cisplatin up to five times against all investigated cancer cell lines; however, no significant selectivity was achieved. The complex induced apoptotic cell death at low micromolar concentrations (0.5 μM for A2780 and HEK293; 2 μM for SK-OV-3 and MDA-MB-231).

KEYWORDS
anticancer activity, glucose derivatives, ruthenium complexes, tetrazene ligands

V. Hamala and A. Martišová contributed equally to this study.

1 | INTRODUCTION

Cancer still remains one of the main health problems worldwide, although successful early case detection combined with new therapeutic options led to almost 30% decrease in overall mortality within the past 25 years.[1] The success in cancer treatment by platinum-based drugs (mainly cisplatin *cis*-[$PtCl_2(NH_3)_2$]) led to an enormous interest in other metal-based drugs (so-called metallodrugs). Among others, ruthenium complexes played a dominant role, whereas $(ImH)^+$[*trans*-$RuCl_4$(κ-*S*-dmso)(κ-*S*-Im)]$^-$ (NAMI A)[2] and [(η^6-arene)$RuCl_2$(pta)][3] (RAPTA, pta = l,3,5-triaza-7-phosphatricyclo[3.3.1.1]decane) were the most prominent ones. Both complexes exhibited antimetastatic effect against cancer cells, whereas the former even entered phase I and phase II clinical trials (albeit not continuing further due to efficiency under expectations). In addition, several other types of highly cytotoxic ruthenium complexes were developed by several laboratories, where $IndH^+$[*trans*-$RuCl_4$(κ-2-*N*-Ind)$_2$]$^-$ (Ind = indazol, KP1039) by Keppler,[4] [(η^6-arene)Ru(en)Cl][PF_6] (en = ethylenediamine) by Sadler,[5] and thiolato-bridged diruthenium complexes by Süss-Fink[6] are representative examples. The effect of organic ligand(s) on the complex cytotoxicity and selectivity was found crucial and widely reviewed.[7–9]

Tetrazene ligands represent a wide family of potentially redox-active ligands, which could adopt three mesomeric forms: neutral tetraazadiene, anionic radical, and dianionic with a central double bond.[10,11] Generally, the ligand is built up directly on a metal center either by insertion of an organic azide into metal–imido bond or by coupling of two organic azides with the evolution of dinitrogen. In the case of ruthenium central atom, the coupling proceeded at the Ru(II) center, that is, Ru(III) is reduced *in situ* by an excess of organic azide, whereas the formed complexes are exclusively diamagnetic irrespective of their geometry. The first ruthenium tetrazene complexes [$RuCl_2(PMe_3)_2${1,4-Mes_2N_4}] (where Mes = mesitylene) and [(η^6-*p*-cymene)Ru{1,4-(R)$MesN_4$}] (where *R* = 2,4,6-*t*-$Bu_3C_4H_2$ or Mes) were synthesized by the reaction of mesityl azide with ruthenium precursors [$RuCl_2(PMe_3)_3$] and [(η^6-*p*-cymene)Ru = *N*(2,4,6-*t*-$Bu_3C_4H_2$)] by Danopoulos et al.[12,13] At the same time, dithiacarbamato ruthenium complex [$Ru(Et_2dtc)_2$(1,4-Ts_2N_4)] (where Et_2dtc = *N*,*N*-diethyldithiocarbamate and Ts = tosyl) was synthesized, which possessed a trigonal prismatic geometry around ruthenium atom.[14] Other tetrazene complexes were identified as by-products generated within azide-alkyne "click" cycloaddition reactions catalyzed by coordinatively unsaturated cyclopentadienyl ruthenium species. Either [Cp*RuCl(COD)] or [Cp*RuCl(*i*-Pr)$_3$] ruthenium precursors (where Cp* = η^5-C_5Me_5, COD = 1,4-cyclooctadiene) reacted with azides $Ph(CH_2)_nN_3$ (*n* = 1, 2) to give the same products [Cp*RuCl{1,4-($(CH_2)_nPh)N_4$}].[15,16] Ruthenium(II) bisamine complex [Cp^RuCl$(NH)_3$] (where Cp^ = η^5-(1-methoxy-2,4-di-*tert*-butyl-3-neopentylcyclopentadienyl)) was successfully used for the synthesis of tetrazenes with pendant arene groups [Cp^RuCl(1,4-R_2N_4)] (where R = Ph,4-$MeOC_4H_4$, 4-$CF_3C_6H_4$) by Park et al.[17] Also Ru(III) precursor [Cp^$RuCl_2]_2$ reacted with various azide derivatives and generated [Cp^RuCl(1,4-R_2N_4)] complexes, where R = Bn[18] and 1-phenylethyl.[19] Surprisingly, the aforementioned reports do not contain any information about the cytotoxicity of ruthenium tetrazene complexes.

Here, we publish the synthesis, characterization, and anticancer properties of a family of ruthenium tetrazene complexes. As our team is interested in the conjugation of carbohydrates with transition metal complexes,[20,21] the main aim of the work was focused on tetrazenes containing glucose or glucosamine moieties on their periphery. Two initial assumptions were used for the introduction of carbohydrate moieties into the tetrazene ligand. The first one was based on the well-known "Warburg effect," that is, high glucose uptake by cancer cells.[22] Second, we proposed to use a glucose moiety as a pattern tailoring lipophilic properties of the whole metallodrug. Therefore, the effect of carbohydrate-protecting *O*-acyl groups on the lipophilicity and cytotoxicity of the ruthenium complex was evaluated.

2 | RESULTS AND DISCUSSION

Starting azides **L1**–**L3b**, **L4a**, and **L5a/b** were purchased from a commercial vendor or prepared by literature methods (for details, see the "Experimental" section). The remaining acetic (**L4b**), propionic (**L3c**, **L4c**), and butyric (**L3d**, **L4d**) acid esters were prepared by esterification of the corresponding azide derivative, as described in Supporting Information.

Ruthenium tetrazene complexes were synthesized according to Scheme 1 under argon atmosphere. A tetrameric structure of precursor [Cp*RuCl]$_4$ was activated by refluxing it in anhydrous acetonitrile. Thus, *in situ*-generated [Cp*Ru$(MeCN)_3$]Cl was reacted with a slightly substoichiometric amount (usually 1.95–1.98 eq.) of the corresponding azide in acetonitrile. The color of the reaction mixture changed almost instantly from orange to green, and gas evolution could be observed in most cases. After evaporation of volatiles, the crude products could be treated/manipulated without inert atmosphere. The products were usually purified using column chromatography on silica gel to obtain the desired products as green solids or waxes.

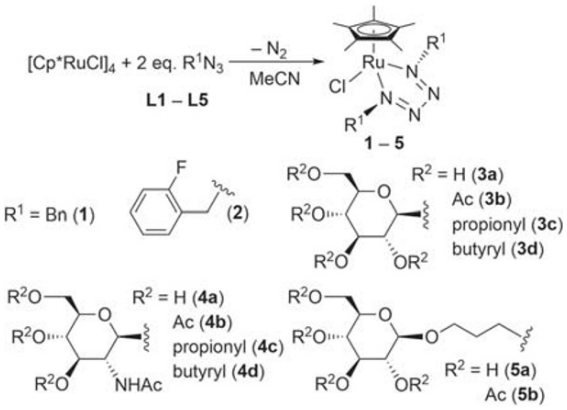

SCHEME 1 Preparation of ruthenium tetrazene complexes **1–5b**

Tetrazenes were obtained in moderate to good yields in the range 22–83%. It is noteworthy that the reaction is tolerant to all functional groups present in the starting azides (*i.e.,* hydroxyl, ester, amide), and we did not observe any transformation/deprotection during the reaction.

In addition to the azide derivatives described earlier, adamantyl azide was subjected to reaction. However, the reaction of the bulky azide with $[Cp^*Ru(MeCN)_3]Cl$ did not lead to a characteristic change in color (from orange to green), and only limited gas evolution was observed (for details, see Supporting Information). After heating of the reaction mixture to reflux, ^1H NMR (nuclear magnetic resonance) spectroscopy exhibited a rather complicated mixture of products. We propose that the bulky adamantyl group precluded the formation of tetrazene framework, as was described previously for the reaction of $[Cp^*RuCl(NH_3)_2]$ with 2,6-diisopropylphenyl azide.[17]

All prepared complexes were characterized by ^1H NMR and ^{13}C NMR, and all the obtained data corroborated the proposed structures. Electrospray ionization–mass spectrometry (ESI–MS) always showed a molecular ion as a $[M + Na]^+$ ion. Coordination of two glucopyranosyl moieties to ruthenium can be easily demonstrated using ^1H NMR spectroscopy. The product formation can be traced according to the characteristic, ~1.2–1.5 ppm, large down-field shift of anomeric protons (in comparison to the starting azide). Moreover, the coordination to ruthenium causes the formation of two sets of signals, each belonging to one of the two nonequivalent glucopyranosyl moieties. The complexes exhibited good stability toward air and water. The stability of **3b** in water solution was investigated in detail. The solution of **3b** in aqueous dmso-d_6 was repeatedly monitored using ^1H NMR spectroscopy for 5 weeks and did not show any deterioration (Figure S1).

2.1 | Molecular structure of 3b

Dark-green crystals suitable for X-ray diffraction analysis were grown by diffusion of the hexane layer into a solution of **3b** in CH_2Cl_2. The species **3b** crystallized in a monoclinic space group $P2_1$ (no. 4) and possessed four symmetrically independent molecules in the crystal structure (Figure S35). Selected geometric parameters are provided in the Supporting Information (Table S1); the molecular structure of one independent molecule and selected bond distances and angles are shown in Figure 1.

Ruthenium possessed a distorted tetrahedral environment, where the chlorine ligand, the centroid of the cyclopentadienyl ring (denoted as Cg), and both terminal nitrogen atoms of the tetrazene ligand were coordinated to the metal center. Ruthenium and four nitrogen atoms of tetrazene constituted almost the ideal plane with a deviation up to 0.064 and 0.055 Å for nitrogen and ruthenium atoms, respectively. The bonding situation in the tetrazene ligand showed comparable values for bonds between nitrogen atoms situated on the lateral (N1–N2 1.318(6)−1.322(6) Å; N3–N4 1.300(6) −1.323(5) Å) and central positions (N2–N3 1.311(5) −1.318(6) Å). This is quite a different situation from previously published tetrazene ruthenium complexes $[RuCl_2(PMe_3)_2\{1,4\text{-}Mes_2N_4\}]$[12] and $[Cp^{\wedge}RuCl(1,4\text{-}R_2N_4)]$ (where R = Ph, Bn),[18] where the former exhibited neutral tetraazadiene property (the difference between the lateral and central bonds was 0.025 and 0.031 Å) and the latter rather asymmetric tetrazene ligand. However, in the case of **3b**, this situation could be affected by the

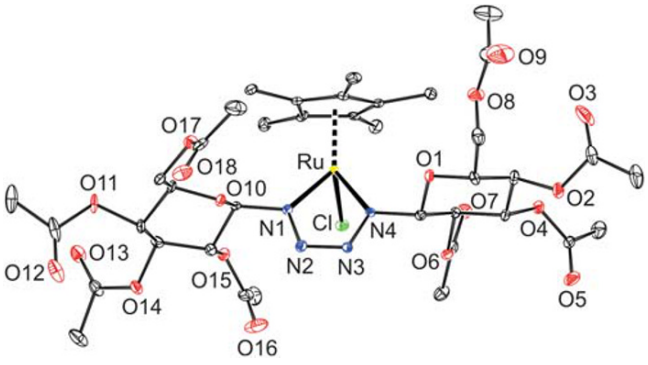

FIGURE 1 Selected molecular structure of **3b** at the 30% probability level with partial labeling. Hydrogen atoms are omitted for clarity. Selected range of bond distances (Å) and angles (°): Ru–Cl 2.343(1)−2.355(1); Ru–Cg 1.875(2)−1.880(2); Ru–N1 1.949(3) −1.967(4); Ru–N4 1.983(4)−1.993(4); N1–N2 1.318(6)−1.322(6); N2–N3 1.311(5)−1.318(6); N3–N4 1.300(6)−1.323(5); Cl–Ru–N1 88.94(13)−96.69(13); Cl–Ru–N4 86.39(12)−92.42(13); N1–Ru–N4 73.22(14)−73.47(17)

presence of either four independent molecules in the structure or bulky glycopyranosyl substituents.

2.2 | Cytotoxicity studies

The cytotoxicity of new compounds against selected cancer cell lines A2780 and SK-OV-3 derived from ovarian cancer, and MDA-MB-231 representing triple negative breast cancer, was evaluated by MTT assay and is presented, together with compound lipophilicity, in Table 1 as IC_{50} values after 72 h incubation. Human embryonal kidney cell line HEK-293 was used to evaluate the effect of tested compounds on noncancerous cells.

Carbohydrate-free complexes **1** and **2** exhibited promising cytotoxicity at low micromolar (7.5 and 4.8 μM) concentrations against cisplatin-sensitive cells A2780 and only about an order of magnitude worse (24 and 54 μM) against intrinsically cisplatin-resistant cell line SK-OV-3.[23] This itself is a reason for further investigation of various tetrazene complexes. However, our main interest lies in carbohydrate-substituted complexes **3**–**5** and particularly in determining how increasing lipophilicity of complexes from unprotected (**3a**, **4a**, **5a**) to butyryl-protected (**3d** and **4d**) ones influences the cytotoxicity. Generally, complexes **3a**, **4a**, and **5a** with unprotected carbohydrate hydroxyls exhibited none or only negligible activity against all studied lines. These results were consistent with the complexes' poor lipophilicity (see Table 1) positioned outside of Lipinski's druggable region (log *P* from −0.4 to 5.6).[24] This indicated the importance of lipophilic functionality in the design of (metalo)drugs, as noted previously.[25,26] However, the situation was less clear for complexes bearing *O*-acyl-protected carbohydrate derivatives, although all of them possessed log *P* values within the region. The complexes exhibited increasing cytotoxicity in the order **3a** ∼ **3d** < **3c** < **3b** for *β*-D-glucopyranosyl-substituted, **4a** ∼ **4b** < **4c** < **4d** for 2-acetamido-*β*-D-glucopyranosyl-substituted, and **5a** < **5b** for propyl *β*-D-glucopyranosides. In this respect, a dramatic decrease in the activity for **3d** should be mentioned, which we tentatively attribute to its decreased aqueous solubility. This result suggests that lipophilicity/aqueous solubility should be well balanced in metallodrug design. The resolution of this problem for **3d** (by the introduction of noncoordinating anion instead of chloride ligand) is currently under investigation.

Among all complexes, three most active ones contained lipophilic propionyl and butyryl groups and followed the order **3c** < **3b** < **4d**, where the most active one exhibited activities substantially higher than cisplatin.

To determine the mechanism of cell death in response to **4d**, the induction of programmed cell death was investigated using Annexin V/PI (prodidium iodide) staining, which enables the detection of both early and late apoptotic cells (Figure 2). Consistent with data from MTT assay, the induction of apoptosis was detected in A2780 and HEK293 cells exposed to lower doses from 0.5 μM of **4d**. In contrast, the induction of apoptotic cell death in SK-OV-3 and MDA-MB-231 cells required higher doses of ∼2 μM of **4d**.

To measure the proliferative capacity of cells exposed to **4d**, we used clonogenic assay (Figure 3). As the graph shows, colony formation in cell culture medium was increasingly inhibited with increasing concentration of

TABLE 1 Tested compounds' lipophilicity (log *P*) and their cytotoxicity (IC_{50}, μM) against cell lines as listed after 72 h treatment

Compound	Log *P*	A2780	SK-OV-3	MDA-MB-231	HEK-293
1	0.6	7.5 ± 0.8	24 ± 3	ND	12 ± 1
2	0.5	4.8 ± 1.3	54 ± 10	ND	26 ± 10
3a	−2.3	65 ± 16	>100	ND	>100
3b	0.9	0.31 ± 0.25	2.5 ± 0.7	ND	0.9 ± 0.4
3c	0.9	0.68 ± 0.21	5.3 ± 0.2	4.3 ± 1.2	1.9 ± 0.8
3d	0.6	>100	>100	>100	>100
4a	−2.4	23 ± 4	>100	ND	58 ± 8
4b	0.3	50 ± 10	>100	>100	>100
4c	1.6	1.49 ± 0.05	14.7 ± 0.8	6.6 ± 2.3	4.2 ± 2.1
4d	0.2	0.36 ± 0.06	2.01 ± 0.21	1.02 ± 0.25	0.60 ± 0.19
5a	−2.4	>100	>100	>100	>100
5b	0.6	29 ± 7	43 ± 8	>100	22 ± 1
Cisplatin	ND	1.7 ± 0.3	5.6 ± 1.0	3.7 ± 0.6	3.8 ± 0.5

Note: ND, not determined.

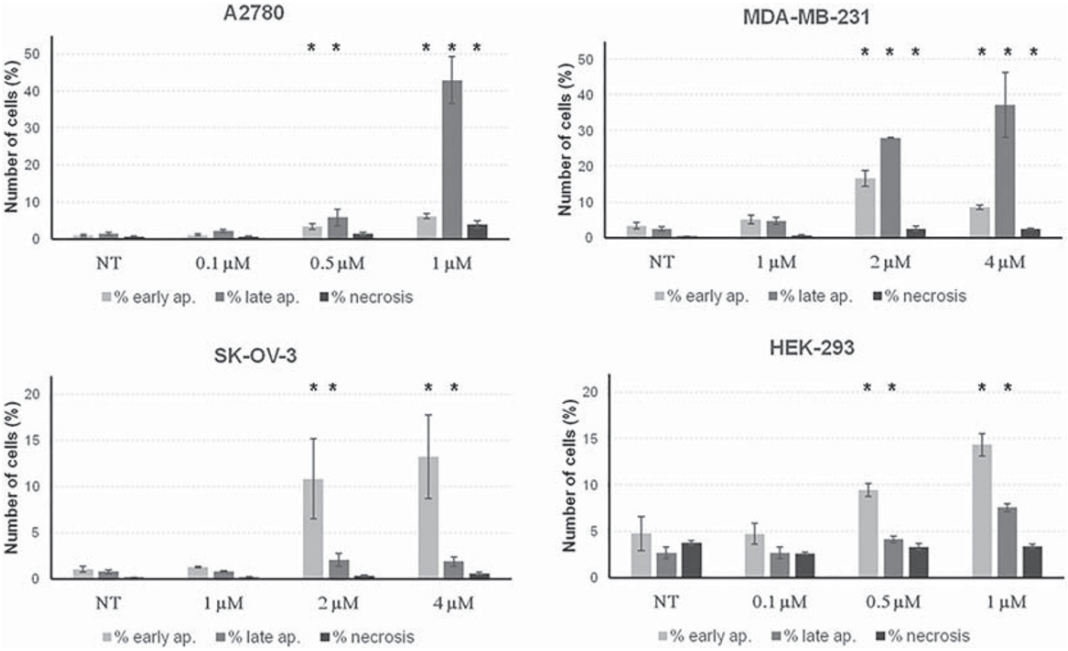

FIGURE 2 Determination of programmed cell death. The graphs were constructed from three independent biological experiments. *, $p < 0.05$, NT represents untreated cells serving as control

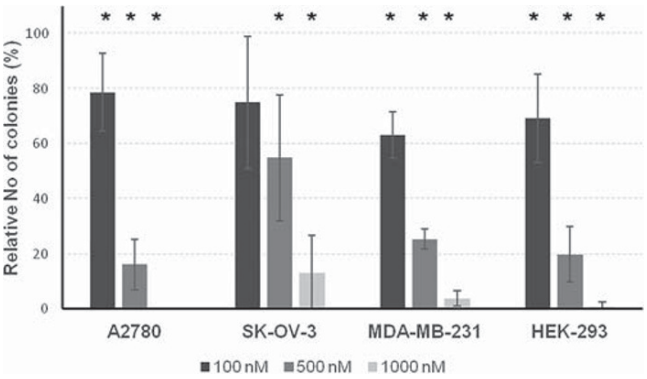

FIGURE 3 Clonogenic assay. Relative numbers of colonies in percentage were calculated with respect to colonies developed from untreated cells. *, $p < 0.05$

4d, but at the same time the ability of particular cell lines to develop colonies after being challenged with **4d** showed the same trend as MTT assay. More sensitive A2780 and HEK-293 cells developed fewer colonies, especially in response to higher doses of **4d**. On the contrary, the most resistant SK-OV-3 cells formed most colonies despite the presence of relatively high doses of **4d** (Figure 3).

The effect of **4d** on cell cycle was also determined. Although SK-OV-3 and MDA-MB-231 showed differences in the fractions of cells in the individual cell-cycle phases compared to A2780 and HEK-293 cells, no significant effect of **4d** on cell-cycle distribution was observed. Similarly, no effect on cell migration of MDA-MB-231 and SK-OV-3 cells exposed to **4d** was observed (data not shown).

3 | CONCLUSIONS

We have shown that various organic azides react smoothly with commercially accessible Ru(II) precursor $[Cp^*RuCl]_4$ after its thermal activation in acetonitrile. The reaction produced air- and water-stable ruthenium tetrazene complexes that could be easily purified using column chromatography on silica. It should be noted that organic azides are popular building blocks widely used in "click chemistry"[27–29] and available from many commercial vendors. Moreover, they could be prepared from primary amines by their reaction with fluorosulfuryl azide, as was demonstrated by more than 1200 examples.[30] Therefore, a large family of ruthenium tetrazene complexes could be quickly synthesized and tested.

The evaluation of *in vitro* cytotoxicity revealed a substantially stronger cytotoxicity for *O*-acyl (propionyl and butyryl) complexes than for unprotected ones. The most active complex **4d** showed IC_{50} values up to five times better compared to cisplatin against all cancer cell lines under study; however, no significant selectivity against cancer cell lines was achieved. The complex induced apoptotic cell death at low micromolar concentrations (0.5 μM for A2780 and HEK293; 2 μM for SK-OV-3; and MDA-MB-231), whereas no significant cell-cycle perturbation was observed.

4 | EXPERIMENTAL

Air-sensitive compounds were manipulated under an argon atmosphere using standard Schlenk techniques. Anhydrous acetonitrile was obtained from Sigma-Aldrich (St. Louis, MO, USA) and stored over MS 3 Å. $[Cp^*RuCl]_4$ was obtained from Strem Chemicals (Newburyport, MA, USA). Benzyl azide (**L1**), 2-fluorobenzyl azide (**L2**), adamantyl azide, and 2,3,4,6-tetra-*O*-acetyl-*β*-D-glucopyranosyl azide (**L3b**) were obtained from Sigma-Aldrich. *β*-D-glucopyranosyl azide (**L3a**),[31] 2-acetamido-2-deoxy-*β*-D-glucopyranosyl azide (**L4a**),[31] 3-azidopropyl-*β*-D-glucopyranoside (**L5a**),[32] and 3-azidopropyl 2-acetamido-2-deoxy-3,4,6-tri-*O*-acetyl-*β*-D-glucopyranoside (**L5b**)[33] were synthesized according to the literature. The synthesis of 2,3,4,6-tetra-*O*-propionyl-*β*-D-glucopyranosyl azide (**L3c**), 2,3,4,6-tetra-*O*-butyryl-*β*-D-glucopyranosyl azide (**L3d**), 2-acetamido-2-deoxy-3,4,6-tri-*O*-acetyl-*β*-D-glucopyranosyl azide (**L4b**), 2-acetamido-2-deoxy-3,4,6-tri-*O*-propionyl-*β*-D-glucopyranosyl azide (**L4c**), and 2-acetamido-2-deoxy-3,4,6-tri-*O*-butyryl-*β*-D-glucopyranosyl azide (**L4d**) is described in the Supporting Information.

^{1}H (400.1/300 MHz), ^{13}C (100.6/75 MHz), and ^{19}F (282 MHz) NMR spectra were measured using a Bruker Avance 400 or Varian Mercury 300 spectrometer at 25 °C. The ^{1}H NMR and ^{13}C NMR spectra were referenced to the solvent signal (δ/ppm; δ_H/δ_C: $CDCl_3$, 7.26/77.16, dmso-d_6, 2.50/39.52; CD_2Cl_2, 5.32/53.84). High-resolution mass spectrometry (HRMS) spectra were measured with a Bruker MicrOTOF-QIII spectrometer using acetonitrile solutions of the samples. The spectrometer was calibrated using sodium formate, and electrospray ionization source in positive mode was used for all analyses. Melting points were determined on a Koffler block and were not corrected.

4.1.1 | General procedure for the preparation of ruthenium tetrazene complexes

$[Cp^*RuCl]_4$ was mixed with dry acetonitrile (c = 0.0125 mol/l) under argon atmosphere, and the suspension was heated by a heat gun until the solid dissolved completely and a transparent orange solution was obtained. Dried ligand (7.8 eq.) was dissolved (or suspended) in dry acetonitrile (c = 0.2 mol/l), and the resulting solution (or suspension) was added dropwise to the stirred solution of the ruthenium precursor. An almost-immediate change in color (orange to green) and gas evolution were observed. The reaction mixture was stirred at room temperature for the desired time, evaporated to dryness, and purified using column chromatography.

4.1.2 | [η^5-(C_5Me_5)RuCl-1,4-κ^2-*N*,*N*′-(1,4-dibenzyltetrazene)] (1)

$[Cp^*RuCl]_4$ (0.136 g, 0.125 mmol) dissolved in 8 ml of acetonitrile was reacted with a solution of benzyl azide (**L1**) in dichloromethane (2.0 ml 0.5 M solution, 1.00 mmol) for 30 min according to the general procedure. Column chromatography (silica gel, eluent tetrahydrofuran [THF]/heptane, 2/5, v/v; R_f = 0.32) produced 0.240 g (79%) of **1** as a green-brown amorphous solid.

4.1.3 | NMR spectra in line with literature[16]

^{1}H NMR (CD_2Cl_2, 300 MHz): 7.39–7.25 (m, 10H, *Ph*), 5.60, 5.36 (2 × d, 2 × 2H, J = 14.1 Hz, CH_2), 1.65 (s, 15H, CH_3 Cp*). ^{13}C{^{1}H} NMR (CD_2Cl_2, 75 MHz): 136.4 (C_{ipso}, Ph), 129.3, 128.6 (2 × 2*C*H, Ph), 127.9 (*C*H, Ph), 100.5 (C_q Cp*), 70.4 (*C*H_2), 10.4 (*C*H_3 Cp*). HRMS–ESI (*m/z*): $[M + Na]^+$, 100%, calculated for $C_{24}H_{29}ClN_4RuNa$ 533.1019; found 533.1017.

4.1.4 | [η^5-(C_5Me_5)RuCl-1,4-κ^2-*N*,*N*′-{1,4-bis(2-fluorobenzyl)tetrazene}] (2)

$[Cp^*RuCl]_4$ (0.189 g, 0.174 mmol) dissolved in 10 ml of acetonitrile was reacted with a solution of 2-fluorobenzyl azide (**L2**) in methyl *tert*-butyl ether (2.5 ml 0.5 M solution, 1.25 mmol) for 3 days according to the general procedure. Evaporation of the reaction mixture produced a crude product, which contained ~5 mol% of 2-fluorobenzaldehyde (singlet at 10.38 ppm characteristic of aldehydic CHO proton).[34] Purification of the crude material using column chromatography (silica gel, eluent dichloromethane, R_f = 0.64) produced **2** as a green solid. Yield 205 mg (64%).

Mp 114 °C. ^{1}H NMR ($CDCl_3$, 300 MHz): 7.31–7.23 (m, 4H, *o*-F-C_6H_4), 7.12–7.06 (m, 4H, *o*-F-C_6H_4), 5.62, 5.40 (2 × d, 2 × 2H, J = 15.2 Hz, CH_2), 1.69 (s, 15H, CH_3 Cp*). ^{13}C{^{1}H} NMR ($CDCl_3$, 75 MHz): 160.4 (d, $^1J_{CF}$ = 246.0 Hz, CF, *o*-F-C_6H_4), 131.7 (d, J_{CF} = 3.8 Hz, CH, *o*-F-C_6H_4), 129.6 (d, J_{CF} = 8.1 Hz, CH, *o*-F-C_6H_4), 124.2 (d, J_{CF} = 3.6 Hz, CH, *o*-F-C_6H_4), 122.9 (d, $^2J_{CF}$ = 14.7 Hz, CCH_2, *o*-F-C_6H_4), 115.2 (d, J_{CF} = 21.6 Hz, CH, *o*-F-C_6H_4), 100.3 (C_q Cp*), 63.1 (d, $^3J_{CF}$ = 3.7 Hz, CH_2), 10.1 (C_q Cp*). ^{19}F NMR ($CDCl_3$, 282 MHz): −117.7 (m, 2F, *o*-*F*-C_6H_4).

4.1.5 | [η⁵-(C_5Me_5)RuCl-1,4-κ²-*N*,*N*′-(1,4-bis(*β*-D-glucopyranosyl)tetrazene)] (3a)

[Cp*RuCl]$_4$ (0.267 g, 0.246 mmol) dissolved in 10 ml of acetonitrile reacted with solid **L3a** (0.393 g, 1.92 mmol) for 48 h. The product precipitated during the reaction from the reaction mixture. Filtration and washing with dry acetonitrile produced **9** as a green dust. Yield 0.479 g (83%).

Mp 130 °C (decomp.). ^{1}H NMR (dmso-d_6, 400 MHz): δ 5.49 (d, 1H, J = 8.4 Hz, H-1′), 5.38 (d, 1H, J = 8.7 Hz, H-1), 5.21 (d, 1H, J = 4.8 Hz, OH-3/4), 5.16–5.13 (m, 3H, OH-3/4, OH-3′, OH-4′), 4.59 (t, 1H, J = 5.7 Hz, OH-6′), 4.52 (t, 1H, J = 5.2 Hz, OH-6), 4.18 (ddd, 1H, J = 8.7, 8.4, 2.9 Hz, H-2′), 3.73–3.59 (m, 5H, H-2, 2H-6, OH-2′, H-6′), 3.51–3.40 (m, 6H, H-3, H-4, H-5, H-3′, H-5′, H-6′), 3.35–3.27 (m, 2H, OH-2, H-4′), 1.75 (s, 15H, CH_3 Cp*). ^{13}C{^{1}H} NMR (dmso-d_6): δ 103.3 (C_q Cp*), 102.3 (C-1), 100.2 (C-1′), 80.3 (C-5′), 80.0 (C-5), 77.3 (C-3′), 76.2 (C-3), 74.8 (C-2′), 74.1 (C-2), 69.8 (C-4′), 69.6 (C-4), 61.0 (C-6′), 60.6 (C-6), 10.2 (CH_3 Cp*). HRMS–ESI (m/z): [M + Na]$^+$, 100%, calculated for $C_{22}H_{37}ClN_4O_{10}RuNa$ 677.1137; found 677.1132.

4.1.6 | [η⁵-(C_5Me_5)RuCl-1,4-κ²-*N*,*N*′-(1,4-bis(2,3,4,6–tetra-*O*-acetyl-*β*-D-glucopyranosyl)tetrazene)] (3b)

[Cp*RuCl]$_4$ (0.256 g, 0.236 mmol) dissolved in 10 ml of acetonitrile reacted with **L3b** (745 mg, 2.00 mmol) dissolved in the same solvent (20 ml) according to the general procedure. Column chromatography (silica gel, eluent dichloromethane:THF 1:4, R_f = 0.89) produced **3b** as a green amorphous solid. Yield 0.774 g (82%).

Mp 124 °C (decomp.). ^{1}H NMR (dmso-d_6, 400 MHz): δ 6.16 (d, 1H, J = 9.3 Hz, H-1′), 6.06 (dd, 1H, J = 9.3, 8.9 Hz, H-2), 5.85 (d, 1H, J = 8.9 Hz, H-1), 5.70 (dd, 1H, J = 9.8, 9.3 Hz, H-3), 5.53 (dd, 1H, J = 9.4, 9.3 Hz, H-3′), 5.27 (t, 1H, J = 9.3 Hz, H-2′), 5.19 (dd, 1H, J = 10.3, 9.4 Hz, H-4′), 5.08 (t, 1H, J = 9.8 Hz, H-4), 4.51 (ddd, 1H, J = 9.8, 6.2, 2.3 Hz, H-5), 4.43 (ddd, 1H, J = 10.3, 4.6, 2.2 Hz, H-5′), 4.28 (dd, 1H, J = 12.4, 4.6 Hz, H-6′), 4.09 (dd, 1H, J = 12.4, 6.2 Hz, H-6), 4.03 (dd, 1H, J = 12.4, 2.3 Hz, H-6), 3.97 (dd, 1H, J = 12.4, 2.2 Hz, H-6′), 2.04, 2.03, 2.00 (3 × s, 3 × 3H, CH_3 OAc), 1.95 (2 × s, 2 × 3H, CH_3 OAc), 1.92 (s, 3H, CH_3 OAc), 1.78 (s, 15H, CH_3 Cp*), 1.69, 1.58 (2 × s, 2 × 3H, CH_3 OAc). ^{13}C{^{1}H} NMR (dmso-d_6, 101 MHz): δ 169.9 (CO), 169.8 (2 × CO), 169.7, 169.4, 169.3, 168.28, 168.26 (5 × CO), 103.9 (C_q Cp*), 98.2 (C-1′), 95.9 (C-1), 73.8 (C-3′), 73.3 (C-5′), 73.1 (C-3), 73.0 (C-5), 71.4 (C-2′), 70.2 (C-2), 68.2 (C-4), 67.1 (C-4′), 62.1 (C-6′), 61.3 (C-6), 20.9, 20.8, 20.49, 20.48, 20.44, 20.41, 20.39, 20.3 (8 × CH_3 OAc), 10.0 (CH_3 Cp*). HRMS–ESI (m/z): [M + Na]$^+$, 100%, calculated for $C_{38}H_{53}ClN_4O_{18}RuNa$ 1013.1987; found 1013.1982.

4.1.7 | [η⁵-(C_5Me_5)RuCl-1,4-κ²-*N*,*N*′-(1,4-bis(2,3,4,6–tetra-*O*-propionyl-*β*-D-glucopyranosyl)tetrazene)] (3c)

[Cp*RuCl]$_4$ (0.068 g, 0.063 mmol) reacted with **L3c** (0.201 g, 0.468 mmol) according to the general procedure. Column chromatography (35 g silica gel, eluent PE:EtOAc 2:1, R_f = 0.22) produced **3c** as a green gel. Yield 0.195 g (70%).

^{1}H NMR (dmso-d_6, 400 MHz): δ 6.17 (d, 1H, J = 9.4 Hz, H-1′), 6.09 (dd, 1H, J = 9.5, 8.9 Hz, H-2), 5.85 (d, 1H, J = 8.9 Hz, H-1), 5.73 (t, 1H, J = 9.5 Hz, H-3), 5.56 (t, 1H, J = 9.4 Hz, H-3′), 5.27 (t, 1H, J = 9.4 Hz, H-2′), 5.22 (dd, 1H, J = 10.2, 9.4 Hz, H-4′), 5.10 (dd, 1H, J = 10.0, 9.5 Hz, H-4), 5.53 (ddd, 1H, J = 10.0, 6.2, 2.2 Hz, H-5), 4.45 (ddd, 1H, J = 10.2, 4.5, 2.2 Hz, H-5′), 4.31 (dd, 1H, J = 12.7, 4.5 Hz, H-6′), 4.11 (dd, 1H, J = 12.4, 6.2 Hz, H-6), 4.03–3.94 (m, 2H, H-6, H-6′), 2.38–2.15 (m, 12H, CH_2CH_3), 2.08–1.84 (m, 4H, CH_2CH_3), 1.77 (s, 15H, CH_3 Cp*), 1.08–0.93 (m, 18H, CH_3), 0.75, 0.73 (2 × t, 2 × 3H, J = 7.5 Hz, CH_3). ^{13}C{^{1}H} NMR (dmso-d_6, 101 MHz): δ 173.2 (2 × CO), 173.1, 173.0, 172.7, 172.6, 171.6, 171.5 (6 × CO), 103.9 (C_q Cp*), 98.4 (C-1′), 95.8 (C-1), 73.7 (C-3′), 73.4 (C-5′), 73.1 (C-3), 73.0 (C-5), 71.3 (C-2′), 70.1 (C-2), 68.0 (C-4), 66.9 (C-4′), 62.0 (C-6), 61.2 (C-6′), 27.0, 26.93, 26.85, 26.83, 26.81, 26.75, 26.64, 26.56 (8 × OCH_2CH_3), 10.0 (CH_3 Cp*), 9.00, 8.97, 8.9, 8.81 (4 × CH_2CH_3), 8.8 (2 × CH_2CH_3), 8.5, 8.4 (2 × CH_2CH_3). HRMS–ESI (m/z): [M + Na]$^+$, 100%, calculated for $C_{46}H_{69}ClN_4O_{18}RuNa$ 1125.3241; found 1125.3240.

4.1.8 | [η⁵-(C_5Me_5)RuCl-1,4-κ²-*N*,*N*′-(1,4-bis(2,3,4,6–tetra-*O*-butyryl-*β*-D-glucopyranosyl)tetrazene)] (3d)

[Cp*RuCl]$_4$ (0.080 g, 0.074 mmol) reacted with **L3d** (0.280 g, 0.577 mmol) according to the general procedure. Column chromatography (45 g silica gel, eluent PE:EtOAc 5:2, R_f = 0.34) produced **3d** as green gel. Yield 0.276 g (77%).

^{1}H NMR (dmso-d_6, 400 MHz): δ 6.14 (d, 1H, J = 9.4 Hz, H-1′), 6.09 (dd, 1H, J = 9.5, 8.8 Hz, H-2), 5.83 (d, 1H, J = 8.8 Hz, H-1), 5.74 (t, 1H, J = 9.5 Hz, H-3), 5.59 (dd, 1H, J = 9.7, 9.1 Hz, H-3′), 5.35 (dd, 1H, J = 9.4, 9.1 Hz, H-2′), 5.21 (dd, 1H, J = 10.2, 9.7 Hz, H-4′), 5.11 (dd, 1H, J = 10.0, 9.5 Hz, H-4), 5.51 (ddd, 1H, J = 10.0, 5.2, 2.8 Hz, H-5), 4.44 (ddd, 1H, J = 10.2, 4.6, 2.2 Hz, H-5′), 4.26 (dd, 1H, J = 12.7, 4.6 Hz, H-6′), 4.06–4.00 (m, 2H, H-6), 3.94 (dd, 1H, J = 12.7, 2.2 Hz, H-6′), 2.35–2.12 (m, 12H, OCH_2CH_2), 2.03–1.81 (m,

4H, OCH_2CH_2), 1.77 (s, 15H, CH_3 Cp*), 1.57–1.42 (m, 12H, OCH_2CH_2), 1.30–1.20 (m, 4H, OCH_2CH_2), 0.89–0.81 (m, 18H, CH_3), 0.69 (t, 3H, J = 7.5 Hz, CH_2CH_3), 0.67 (t, 3H, J = 7.4 Hz, CH_2CH_3). $^{13}C\{^1H\}$ NMR (dmso-d_6, 101 MHz): δ 172.28, 172.27, 172.1, 172.0, 171.7, 171.56, 170.62, 170.59 (8 × CO), 103.9 (C_q Cp*), 98.2 (C-1′), 95.8 (C-1), 73.6 (C-3′), 73.5 (C-5′), 73.0 (C-5), 72.9 (C-3), 71.0 (C-2′), 70.0 (C-2), 68.0 (C-4), 67.1 (C-4′), 61.8 (C-6), 61.2 (C-6′), 35.5, 35.4, 35.3, 35.24, 35.17, 35.13, 35.10, 35.05 (8 × OCH_2CH_2), 17.8, 17.73 (2 × CH_2CH_3), 17.70 (2 × CH_2CH_3), 17.68, 17.5, 17.3, 17.2 (4 × CH_2CH_3), 13.30 (2 × CH_2CH_3), 13.31 (CH_2CH_3), 13.30 (2 × CH_2CH_3), 13.28, 13.25, 13.2 (3 × CH_2CH_3), 10.0 (CH_3 Cp*). HRMS–ESI (m/z): $[M + Na]^+$, 100%, calculated for $C_{54}H_{85}ClN_4O_{18}RuNa$ 1237.4495; found 1237.4489.

4.1.9 | [η⁵-(C_5Me_5)RuCl-1,4-κ²-*N*,*N*′-(1,4-bis(2-acetamido-2-deoxy-*β*-D-glucopyranosyl)tetrazene)] (4a)

$[Cp^*RuCl]_4$ (0.238 g, 0.270 mmol) reacted with **L4a** (0.518 g, 2.10 mmol) according to the general procedure. The product was precipitated from the reaction mixture, filtered, and washed with dry THF producing **4a** as a green powder. Yield 0.563 g (71%).

Mp 124 °C (decomp.). ^1H NMR (dmso-d_6, 400 MHz): δ 7.18 (d, 1H, J = 8.2 Hz, NH), 6.59 (brs, 1H, NH′), 5.97 (d, 1H, J = 9.5 Hz, H-1′), 5.87 (d, 1H, J = 9.3 Hz, H-1), 5.16 (d, 1H, J = 5.5 Hz, OH-3′), 5.11 (d, 1H, J = 5.5 Hz, OH-4), 5.09 (d, 1H, J = 5.7 Hz, OH-4′), 5.03 (d, 1H, J = 5.3 Hz, OH-3), 4.57 (t, 1H, J = 5.7 Hz, OH-6), 4.46 (ddd, 1H, J = 9.3, 9.1, 8.2 Hz, H-2), 4.41 (ddd, 1H, J = 9.1, 8.9, 5.5 Hz, H-3′), 4.26 (brs, 1H, OH-6′), 3.86 (ddd, 1H, J = 9.4, 9.1, 5.3 Hz, H-3), 3.76–3.66 (m, 2H, H-6, H-6′), 3.62–3.41 (m, 5H, H-5, H-6, H-2′, H-5′, H-6′), 3.32–3.25 (m, 2H, H-4, H-4′), 1.72 (s, 15H, CH_3 Cp*), 1.57, 1.51 (2 × s, 2 × 3H, CH_3 NHAc). $^{13}C\{^1H\}$ NMR (dmso-d_6, 101 MHz): δ 170.1, 169.2 (2 × CO), 102.5 (C_q Cp*), 97.7 (C-1′), 97.6 (C-1), 80.2 (C-5), 79.8 (C-5′), 74.2 (C-3), 72.0 (C-3′), 71.0 (C-4′), 70.8 (C-4), 61.1 (C-6′), 61.0 (C-6), 59.0 (C-2′), 56.0 (C-2), 23.8, 23.4 (2 × CH_3 NHAc), 10.3 (CH_3 Cp*). HRMS–ESI (m/z): $[M + Na]^+$, 100%, calculated for $C_{26}H_{43}ClN_6O_{10}RuNa$ 759.1669; found 759.1664.

4.1.10 | [η⁵-(C_5Me_5)RuCl-1,4-κ²-*N*,*N*′-(1,4-bis(2-acetamido-2-deoxy-3,4,6–tri-*O*-acetyl-*β*-D-glucopyranosyl)tetrazene)] (4b)

$[Cp^*RuCl]_4$ (0.134 g, 0.123 mmol) reacted with **L4b** (0.358 g, 0.96 mmol) according to the general procedure. Column chromatography (30 g silica gel, eluent EtOAc: THF 4:1, R_f = 0.42) produced **4b** as a green amorphous solid. Yield 0.270 g (56%).

^1H NMR (dmso-d_6, 400 MHz): δ 7.26 (d, 1H, J = 8.2 Hz, NH), 6.89 (d, 1H, J = 6.4 Hz, NH′), 6.21 (d, 1H, J = 9.5 Hz, H-1′), 6.12 (d, 1H, J = 9.3 Hz, H-1), 5.93 (t, 1H, J = 9.7 Hz, H-3′), 5.70 (t, 1H, J = 9.8 Hz, H-3), 5.06 (dd, 1H, J = 9.7, 9.4 Hz, H-4′), 5.02 (dd, 1H, J = 9.8, 9.4 Hz, H-4), 4.80 (ddd, 1H, J = 9.8, 9.3, 8.2 Hz, H-2), 4.33 (dd, 1H, J = 12.6, 4.7 Hz, H-6′), 4.23–4.11 (m, 3H, H-5, H-6, H-5′), 4.03–3.95 (m, 3H, H-6, H-2′, H-6′), 2.03, 2.01, 2.00 (3 × s, 3 × 3H, CH_3 OAc), 1.96 (s, 2 × 3H, CH_3 OAc), 1.93 (s, 3H, CH_3 OAc), 1.76 (s, 15H, CH_3 Cp*), 1.51, 1.48 (2 × s, 2 × 3H, CH_3 NHAc). $^{13}C\{^1H\}$ NMR (dmso-d_6, 101 MHz): δ 170.0, 169.94, 169.91, 169.6, 169.5, 169.42, 169.39, 169.1 (8 × CO), 103.4 (C_q Cp*), 97.3 (C-1′), 96.3 (C-1), 73.7 (C-5′), 73.5 (C-5), 72.7 (C-3), 71.6 (C-3′), 68.8 (C-4), 68.4 (C-4′), 62.2 (C-6), 61.6 (C-6′), 55.2 (C-2′), 53.3 (C-2), 23.3, 22.9 (2 × CH_3 NHAc), 20.54, 20.51, 20.48, 20.46, 20.44, 20.42 (6 × CH_3 OAc), 10.2 (CH_3 Cp*). HRMS–ESI (m/z): $[M + Na]^+$, 100%, calculated for $C_{38}H_{55}ClN_6O_{16}RuNa$ 1011.2306; found 1011.2311.

4.1.11 | [η⁵-(C_5Me_5)RuCl-1,4-κ²-*N*,*N*′-(1,4-bis(2-acetamido-2-deoxy-3,4,6–tri-*O*-propionyl-*β*-D-glucopyranosyl)tetrazene)] (4c)

$[Cp^*RuCl]_4$ (0.087 g, 0.080 mmol) reacted with **L4c** (0.258 g, 0.623 mmol) according to the general procedure. Column chromatography (40 g silica gel, eluent EtOAc, R_f = 0.44) produced **4c** as a green amorphous solid. Yield 0.125 g (36%).

^1H NMR (dmso-d_6, 400 MHz): δ 7.25 (d, 1H, J = 8.4 Hz, NH), 6.92 (d, 1H, J = 7.4 Hz, NH′), 6.18 (d, 1H, J = 9.6 Hz, H-1′), 6.11 (d, 1H, J = 9.3 Hz, H-1), 5.92 (t, 1H, J = 9.7 Hz, H-3′), 5.71 (t, 1H, J = 9.8 Hz, H-3), 5.09 (t, 1H, J = 9.7 Hz, H-4′), 5.04 (t, 1H, J = 9.8 Hz, H-4), 4.81 (ddd, 1H, J = 9.8, 9.3, 8.4 Hz, H-2), 4.37 (dd, 1H, J = 12.6, 4.7 Hz, H-6′), 4.27–4.19 (m, 2H, H-5, 5′), 4.17 (dd, 1H, J = 12.4, 6.0 Hz, H-6), 4.08 (ddd, 1H, J = 9.7, 9.6, 7.4 Hz, H-2′), 4.02 (dd, 1H, J = 12.4, 1.8 Hz, H-6), 3.96 (dd, 1H, J = 12.6, 2.0 Hz, H-6′), 2.33–2.16 (m, 12H, CH_2CH_3), 1.76 (s, 15H, CH_3 Cp*), 1.50, 1.47 (2 × s, 2 × 3H, CH_3 NHAc), 1.03–0.96 (m, 18H, CH_2CH_3). $^{13}C\{^1H\}$ NMR (dmso-d_6, 101 MHz): δ 173.26, 173.25, 172.9, 172.8, 172.7, 172.6, 169.9, 169.1 (8 × CO), 103.4 (C_q Cp*), 97.4 (C-1′), 96.3 (C-1), 73.8 (C-5′), 73.6 (C-5), 72.6 (C-3), 71.7 (C-3′), 68.6 (C-4), 68.3 (C-4′), 62.1 (C-6), 61.5 (C-6′), 55.0 (C-2′), 53.3 (C-2), 26.91, 26.85, 26.84, 26.81, 26.7, 26.6 (6 × CH_2CH_3), 23.3, 22.9 (2 × CH_3 NHAc), 10.2 (CH_3 Cp*), 9.13, 9.07, 8.94, 8.91 (4 × CH_2CH_3), 8.8 (2 × CH_2CH_3). HRMS–ESI (m/z): $[M + Na]^+$, 100%,

calculated for $C_{44}H_{67}ClN_6O_{16}RuNa$ 1095.3247; found 1095.3253.

4.1.12 | [η^5-(C_5Me_5)RuCl-1,4-κ^2-*N*,*N*′-(1,4-bis(2-acetamido-2-deoxy-3,4,6–tri-*O*-butyryl-*β*-D-glucopyranosyl)tetrazene)] (4d)

$[Cp^*RuCl]_4$ (0.054 g, 0.050 mmol) reacted with **L4d** (0.178 g, 0.390 mmol) according to the general procedure. Column chromatography (40 g silica gel, eluent PE: EtOAc 3:2, $R_f = 0.30$) produced **4d** as a green amorphous solid. Yield 0.145 g (63%).

^{1}H NMR (dmso-d_6, 400 MHz): δ 7.27 (d, 1H, J = 8.4 Hz, NH), 6.89 (d, 1H, J = 7.3 Hz, NH′), 6.19 (d, 1H, J = 9.5 Hz, H-1′), 6.09 (d, 1H, J = 9.3 Hz, H-1), 5.93 (t, 1H, J = 9.8 Hz, H-3′), 5.70 (t, 1H, J = 9.8 Hz, H-3), 5.11 (t, 1H, J = 9.8 Hz, H-4′), 5.06 (t, 1H, J = 9.8 Hz, H-4), 4.82 (ddd, 1H, J = 9.8, 9.3, 8.4 Hz, H-2), 4.32 (dd, 1H, J = 12.7, 4.6 Hz, H-6′), 4.26–4.19 (m, 2H, H-5, 5′), 4.14 (dd, 1H, J = 12.4, 5.6 Hz, H-6), 4.05–4.01 (m, 2H, H-6, H-2′), 3.96 (dd, 1H, J = 12.7, 1.8 Hz, H-6′), 2.30–2.14 (m, 12H, OCH_2CH_2), 1.76 (s, 15H, CH_3 Cp*), 1.55–1.44 (m, 18H, $6OCH_2CH_2$, $2CH_3$ NHAc), 0.88–0.80 (m, 18H, CH_2CH_3). $^{13}C\{^1H\}$ NMR (dmso-d_6, 101 MHz): δ 172.37, 172.36, 171.9, 171.8, 171.7, 171.6, 169.9, 169.0 (8 × CO), 103.4 (C_q Cp*), 97.4 (C-1′), 96.4 (C-1), 73.8 (C-5′), 73.6 (C-5), 72.5 (C-3), 71.5 (C-3′), 68.5 (C-4), 68.2 (C-4′), 61.9 (C-6), 61.5 (C-6′), 55.1 (C-2′), 53.2 (C-2), 35.4, 35.3, 35.24, 35.18, 35.17, 35.1 (6 × OCH_2CH_2), 23.3, 22.9 (2 × CH_3 NHAc), 17.9, 17.83, 17.75, 17.73 (4 × CH_2CH_3), 17.70 (2 × CH_2CH_3), 13.38, 13.37, 13.31 (3 × CH_2CH_3), 13.28 (2 × CH_2CH_3), 13.26 (CH_2CH_3), 10.2 (CH_3 Cp*). HRMS–ESI (*m*/*z*): $[M + Na]^+$, 100%, calculated for $C_{50}H_{79}ClN_6O_{16}RuNa$ 1179.4188; found 1179.4187.

4.1.13 | [η^5-(C_5Me_5)RuCl-1,4-κ^2-*N*,*N*′-(1,4-bis(3-(*β*-D-glucopyranosyl)-propyl) tetrazene)] (5a)

$[Cp^*RuCl]_4$ (0.360 g, 0.332 mmol) reacted with **L5a** (0.684 g, 2.59 mmol) overnight according to the general procedure. Column chromatography (20 g silica gel, eluent acetone:EtOH 10:1, $R_f = 0.80$) produced **5a** as a green foam. Yield 0.154 g (22%).

^{1}H NMR (dmso-d_6, 400 MHz): δ 4.99, 4.98 (2 × d, 2 × 1H, J = 4.5 Hz, OH), 4.93 (d, 2H, J = 4.5 Hz, OH), 4.89 (d, 2H, J = 4.5 Hz, OH), 4.50–4.40 (m, 4H, 2OH, 2NCHH), 4.34–4.25 (m, 2H, NCHH), 4.18, 4.16 (2 × d, 2 × 1H, J = 7.7 Hz, H-1), 3.89–3.82 (m, 2H, OCHH), 3.69–3.65 (m, 2H, H-6), 3.61–3.49 (m, 2H, OCHH), 3.46–3.41 (m, 2H, H-6), 3.15–2.96 (m, 8H, H-2, H-3, H-4, H-5), 2.33–2.29, 2.16–2.08 (2 × m, 2 × 2H, CHH), 1.69 (s, 15H, CH_3 Cp*). $^{13}C\{^1H\}$ NMR (dmso-d_6, 101 MHz): δ 103.0, 102.8 (2 × C-1), 99.4 (C_q Cp*), 76.8 (2C-3, 2C-5), 73.6, 73.5 (2 × C-2), 70.12, 70.09 (2 × C-4), 66.61, 66.56 (2 × OCH_2), 63.7, 63.5 (2 × NCH_2), 61.13, 61.10 (2 × C-6), 29.2, 29.1 (2 × CH_2), 9.6 (CH_3 Cp*). HRMS–ESI (*m*/*z*): $[M + Na]^+$, 100%, calculated for $C_{28}H_{49}ClN_4O_{12}RuNa$ 793.1976; found 793.1981.

4.1.14 | [η^5-(C_5Me_5)RuCl-1,4-κ^2-*N*,*N*′-(1,4-bis(3-(2,3,4,6-tetra-*O*-acetyl-*β*-D-glucopyranosyl)-propyl)tetrazene)] (5b)

$[Cp^*RuCl]_4$ (0.178 g, 0.164 mmol) reacted with **L5b** (0.600 g, 1.39 mmol) overnight according to the general procedure. Column chromatography (20 g silica gel, eluent hexane:EtOAc 1:3, $R_f = 0.70$) produced **5b** as a green solid. Yield 0.451 g (62%).

Mp 64 °C. ^{1}H NMR (dmso-d_6, 400 MHz): δ 5.28, 5.27 (2 × dd, 2 × 1H, J = 9.8, 9.4 Hz, H-3), 4.90 (t, 2H, J = 9.8 Hz, H-4), 4.82–4.78 (m, 4H, H-1, H-2), 4.42–4.31 (m, 2H, NCHH), 4.23–4.14 (m, 4H, NCHH, H-6), 4.04–3.97 (m, 4H, H-6, H-5), 3.84–3.75 (m, 2H, OCHH), 3.63–3.54 (m, 1H, OCHH), 3.45–3.39 (m, 1H, OCHH), 2.32–2.13 (m, 4H, CHH), 2.02, 2.01, 1.98 (3 × s, 3 × 6H, CH_3 OAc), 1.95, 1.94 (2 × s, 2 × 3H, CH_3 OAc), 1.67 (s, 15H, CH_3 Cp*). $^{13}C\{^1H\}$ NMR (dmso-d_6, 101 MHz): δ 170.0 (2 × CO-6), 169.6 (2 × CO-3), 169.3 (2 × CO-4), 169.2, 169.1 (2 × CO-2), 99.54 (C-1), 99.46 (C_q Cp*), 99.4 (C-1), 72.1, 72.0 (2 × C-3), 71.01, 70.97 (2 × C-2), 70.6, 70.5 (2 × C-5), 68.2 (2 × C-4), 67.4, 67.0 (2 × OCH_2), 63.2, 62.8 (2 × NCH_2), 61.8 (2 × C-6), 28.8, 28.7 (2 × CH_2), 20.5, 20.4 (2 × 3 CH_3 OAc), 20.3 (2 × CH_3 OAc), 9.5 (CH_3 Cp*). HRMS–ESI (*m*/*z*): $[M + Na]^+$, 100%, calculated for $C_{44}H_{65}ClN_4O_{20}RuNa$ 1129.2826; found 1129.2826.

4.2 | X-ray crystallography

Diffraction data for **3b** were collected on a Bruker D8 VENTURE diffractometer (Mo-Kα radiation, λ = 0.71073 Å) at 150 K using an Oxford Cryostream cooler. The collected data were reduced using the diffractometer software. The phase problem was solved by intrinsic phasing, and structure models were refined by full-matrix least squares on F^2 (SHELX-2018/3).[35] All non-hydrogen atoms were refined anisotropically. Hydrogen atoms were placed in idealized positions and refined isotropically using the riding model. Solvent molecules present in the structure could not be refined with satisfactory results, and their contribution to diffraction data was subtracted using the SQUEEZE procedure

implemented in PLATON.[36] Molecular graphics was performed using the PLATON program.

CCDC 1979972 contains supplementary crystallographic data deposited for **3b**. These data can be obtained free of charge from The Cambridge Crystallographic Data Centre at www.ccdc.cam.ac.uk/data_request/cif.

4.3 | Cell lines and cytotoxicity testing

All human cells were maintained at 37 °C in humidified atmosphere with 5% CO_2. A2780 cells were grown in high-glucose RPMI-1640 and SK-OV-3 cells in McCoy's 5ª, and HEK 293 and MDA-MB-231 cells were maintained in high-glucose Dulbecco's modified Eagle's medium (DMEM, all media were from Sigma-Aldrich (St. Louis, MO, USA)). Each media was supplemented with 10% fetal bov

ine serum (Gibco, ThermoFisher Scientific, Waltham, MA, USA), 300 μg/ml of L-glutamine (Sigma-Aldrich), and 100 μg/ml of HyClone Penicillin–Streptomycin 100X solution (BioSera, Nuaille, France). The culture medium was changed during each cell passage every 2–3 days. Cells were grown to 60–80% confluence before experimental treatments with tested compounds at concentrations from 1 to 100 μM. Cells were mycoplasma free throughout the experiments.

Cells were seeded in a 96-well plate at a density of 3000 cells/well for cytotoxicity testing. The next day, these cells were exposed to selected compounds for 72 h. The cell viability was measured using colorimetric MTT assay as described previously.[37] Data from MTT assay were analyzed in GraphPad Prism software and expressed as IC_{50} values (compound concentrations that produce 50% of cell metabolic inhibition). All experiments were performed independently at least thrice.

4.4 | Clonogenic assay

A total of 200 cells per well were seeded in six-well plates, and next day these cells were treated with **4d** at 100-, 500- and 1000-nM concentration. Ten days later, the cells were washed twice with phosphate-buffered saline (PBS) and fixed for 30 min in methanol, and developed colonies were then visualized using Giemsa–Romanowski staining and counted.

4.5 | Determination of partition coefficient (log *P*) by "shake flask" method

The tested compounds were dissolved at 20-mM concentration in dimethyl sulfoxide. Particular stocks were added to water and 1-octanol to a final concentration of 1 mM. The same volumes of water and octanol containing the same complex were equally mixed and shaken for 5 min. Then the tubes were shortly spun, and samples from aqueous and organic layers were subjected to UV–Vis. spectrophotometry (NanoDrop 2000, ThermoFisher Scientific). Absolute amounts of individual complexes were calculated by constructing respective calibration curves (data not shown). Log *P* was defined as the logarithm of the ratio of the concentrations of a solute between the two solvents.

4.6 | Cell-cycle determination

Cells (2×10^5) were seeded in six-well plates and treated with 0.1, 0.5, or 1 μM **4d** for 48 h. The cells were then washed twice with PBS and fixed in 70% ethanol overnight at 4 °C. After incubation, the cells were washed with PBS and stained with 1 ml of PI staining solution per sample (0.1% Triton X-100, 10 μg/ml propidium iodide, 100 μg/ml DNAse-free RNAase A, Sigma-Aldrich) for 30 min at room temperature in the dark. After incubation, the fluorescence was measured using a flow cytometer (FACS Verse, BD Biosciences, Franklin Lakes, NJ, USA) and evaluated using BD FACSuite v 1.0.6. In total, 10,000 events per sample were recorded.

4.7 | Annexin V cell death analysis

Cells (10^5) were seeded in 12-well plates, and then A2780 and HEK-293 cells were treated with 0.1, 0.5, and 1 μM of **4d** for 24 h, whereas SK-OV-3 and MDA-MB-231 cells were exposed to 1, 2, and 4 μM of **4d** for 24 h. Then, the cells were collected with Accutase and washed twice with PBS. Cell pellets were then resuspended in 50 μl of staining solution prepared from 1× binding buffer (20× Annexin V Binding Buffer, MACS Miltenyi Biotec), 1 μl of FITC-Annexin V (Biolegends, San Diego, CA, USA), and 0.5 μl of 1 mg/ml PI Sigma-Aldrich (St. Louis, MO, USA) and incubated for 20 min in the dark at room temperature. The fluorescence signal was detected using a flow cytometer (FACS Verse, BD Biosciences). A total of 10,000 events were recorded for each sample. The percentage of apoptotic cells was quantified using FCS Express 4 software (BD Biosciences).

4.8 | Wound healing assay

Confluent cells grown in 12-well plates were scraped with a sterile micropipette tip and then incubated in serum-

free DMEM with 1 and 2 μM of **4d**. Time-lapse acquisition of the wound closure was detected using a Nicon Eclipse Ti-E system at 10× magnification. The pictures were captured at three randomly chosen fields within the wound region every 4 h for 24 h. The migration rate was assessed using TScratch software by quantification of the cell-free area 24 h post-scratching.

4.9 | Statistical analysis

One-way analysis of variance with *post hoc* Tukey HSD calculator was used to determine statistically significant differences between the groups generated from at least three independent experiments unless otherwise stated. It was performed using the free online web tool available at https://astatsa.com/OneWay_Anova_with_TukeyHSD/. Tests with $p < 0.05$ were considered as significant. The error bars represent the standard deviation of the corresponding data sets.

ACKNOWLEDGMENTS

This work was supported by the Czech Science Foundation (Grantová Agentura České Republiky, project number 17-05838S) and Ministry of Health of the Czech Republic (Ministerstvo Zdravotnictví České Republiky, project DRO MMCI, 00209805). The authors thank Dr. Lidmila Petrusová for melting point determinations. Jiří Pinkas thanks Ms. Ivana Dobiášová for assistance in the preparation of **5a** and **5b**.

CONFLICT OF INTEREST

The authors declare no competing financial interest.

FUNDING INFORMATION

This work was supported by the Czech Science Foundation (project number 17-05838S) and Ministry of Health of the Czech Republic (project DRO MMCI, 00209805).

ORCID

Jiří Pinkas https://orcid.org/0000-0003-3478-0802

REFERENCES

[1] R. L. Siegel, K. D. Miller, A. Jemal, *CA: Cancer J. Clin.* **2020**, *70*, 7.
[2] E. Alessio, *Eur. J. Inorg. Chem.* **2017**, *2017*, 1549.
[3] B. S. Murray, M. V. Babak, C. G. Hartinger, P. J. Dyson, *Coord. Chem. Rev.* **2016**, *306*, 86.
[4] C. G. Hartinger, S. Zorbas-Seifried, M. A. Jakupec, B. Kynast, H. Zorbas, B. K. Keppler, *J. Inorg. Biochem.* **2006**, *100*, 891.
[5] H. Chen, J. A. Parkinson, S. Parsons, R. A. Coxall, R. O. Gould, P. J. Sadler, *J. Am. Chem. Soc.* **2002**, *124*, 3064.
[6] J. Furrer, G. Süss-Fink, *Coord. Chem. Rev.* **2016**, *309*, 36.
[7] A. Levina, A. Mitra, P. A. Lay, *Metallomics* **2009**, *1*, 458.
[8] T. S. Morais, A. Valente, A. I. Tomaz, F. Marques, M. H. Garcia, *Future Med. Chem.* **2016**, *8*, 527.
[9] P. Zhang, P. J. Sadler, *J. Organomet. Chem.* **2017**, *839*, 5.
[10] D. S. Moore, S. D. Robinson, *Adv. Inorg. Chem.* **1986**, *30*, 1.
[11] W. C. Trogler, *Acc. Chem. Res.* **1990**, *23*, 426.
[12] A. A. Danopoulos, R. S. HayMotherwell, G. Wilkinson, S. M. Cafferkey, T. K. N. Sweet, M. B. Hursthouse, *J. Chem. Soc., Dalton Trans.* **1997**, 3177.
[13] A. A. Danopoulos, G. Wilkinson, T. K. N. Sweet, M. B. Hursthouse, *J. Chem. Soc., Dalton Trans.* **1996**, 3771.
[14] W.-H. Leung, J. L. C. Chim, H. Hou, T. S. M. Hun, I. D. Williams, W.-T. Wong, *Inorg. Chem.* **1997**, *36*, 4432.
[15] B. C. Boren, S. Narayan, L. K. Rasmussen, L. Zhang, H. T. Zhao, Z. Y. Lin, G. C. Jia, V. V. Fokin, *J. Am. Chem. Soc.* **2008**, *130*, 8923.
[16] M. Lamberti, G. C. Fortman, A. Poater, J. Broggi, A. M. Z. Slawin, L. Cavallo, S. P. Nolan, *Organometallics* **2012**, *31*, 756.
[17] J. Y. Park, Y. Kim, D. Y. Bae, Y. H. Rhee, J. Park, *Organometallics* **2017**, *36*, 3471.
[18] J. Risse, R. Scopelliti, K. Severin, *Organometallics* **2011**, *30*, 3412.
[19] H. K. Pak, J. Han, M. Jeon, Y. Kim, Y. Kwon, J. Y. Park, Y. H. Rhee, J. Park, *ChemCatChem* **2015**, *7*, 4030.
[20] T. Hodik, M. Lamac, L. C. St'astna, J. Karban, L. Koubkova, R. Hrstka, I. Cisarova, J. Pinkas, *Organometallics* **2014**, *33*, 2059.
[21] M. Lamac, M. Horacek, L. C. Stastna, J. Karban, L. Sommerova, H. Skoupilova, R. Hrstka, J. Pinkas, *Appl. Organomet. Chem.* **2020**, *34*, e5318.
[22] D. Hanahan, R. A. Weinberg, *Cell* **2011**, *144*, 646.
[23] C. M. Beaufort, J. C. Helmijr, A. M. Piskorz, M. Hoogstraat, K. Ruigrok-Ritstier, N. Besselink, M. Murtaza, W. F. J. van IJcken, A. A. J. Heine, M. Smid, M. J. Koudijs, J. D. Brenton, E. M. J. J. Berns, J. Helleman, *PLoS ONE* **2014**, *9*, e103988.
[24] C. A. Lipinski, F. Lombardo, B. W. Dominy, P. J. Feeney, *Adv. Drug Delivery Rev.* **2001**, *46*, 3.
[25] C. T. Campbell, U. Aich, C. A. Weier, J. J. Wang, S. S. Choi, M. M. Wen, K. Maisel, S. G. Sampathkumar, K. J. Yarema, *J. Med. Chem.* **2008**, *51*, 8135.
[26] S. M. Meier-Menches, C. Gerner, W. Berger, C. G. Hartinger, B. K. Keppler, *Chem. Soc. Rev.* **2018**, *47*, 909.
[27] P. Thirumurugan, D. Matosiuk, K. Jozwiak, *Chem. Rev.* **2013**, *113*, 4905.
[28] E. Kim, H. Koo, *Chem. Sci.* **2019**, *10*, 7835.
[29] X. Y. Jiang, X. Hao, L. L. Jing, G. C. Wu, D. W. Kang, X. Y. Liu, P. Zhan, *Expert Opin. Drug Discov.* **2019**, *14*, 779.
[30] G. Meng, T. Guo, T. Ma, J. Zhang, Y. Shen, K. B. Sharpless, J. Dong, *Nature* **2019**, *574*, 86.
[31] T. Tanaka, H. Nagai, M. Noguchi, A. Kobayashi, S. Shoda, *Chem. Commun.* **2009**, 3378.
[32] A. K. Yadav, D. L. Shen, X. Shan, X. He, A. R. Kermode, D. J. Vocadlo, *J. Am. Chem. Soc.* **2015**, *137*, 1181.
[33] K. Huang, F. Parmeggiani, H. Ledru, K. Hollingsworth, J. M. Pons, A. Marchesi, P. Both, A. P. Mattey, E. Pallister, G. S. Bulmer, J. M. van Munster, W. B. Turnbull, M. C. Galan, S. L. Flitsch, *Org. Biomol. Chem.* **2019**, *17*, 5920.
[34] Y. Corre, V. Rysak, X. Trivelli, F. Agbossou-Niedercorn, C. Michon, *Eur. J. Org. Chem.* **2017**, *2017*, 4820.
[35] G. M. Sheldrick, *Acta Crystallogr. Sect. C-Struct. Chem.* **2015**, *C71*, 3.

[36] A. L. Spek, *Acta Crystallogr. Sect. D-Biol. Crystallogr.* **2009**, *D65*, 148.
[37] T. Hodik, M. Lamac, L. C. Stastna, P. Curinova, J. Karban, H. Skoupilova, R. Hrstka, I. Cisarova, R. Gyepes, J. Pinkas, *J. Organomet. Chem.* **2017**, *846*, 141.

SUPPORTING INFORMATION

Additional supporting information may be found online in the Supporting Information section at the end of this article.

How to cite this article: Hamala V, Martišová A, Červenková Šťastná L, et al. Ruthenium tetrazene complexes bearing glucose moieties on their periphery: Synthesis, characterization, and *in vitro* cytotoxicity. *Appl Organomet Chem*. 2020;e5896. https://doi.org/10.1002/aoc.5896